Environmental Science & Technology

pubs.acs.org/est

Article

Variations in Colloidal DOM Composition with Molecular Weight within Individual Water Samples as Characterized by Flow Field-Flow Fractionation and EEM-PARAFAC Analysis

Hui Lin and Laodong Guo*

Cite This: https://dx.doi.org/10.1021/acs.est.9b07123

Read Online

ACCESS | Metrics & More | Article Recommendations | Supporting Information

ABSTRACT: Fluorescence excitation emission matrices (EEM) and parallel factor (PARAFAC) analysis have been widely used in the characterization of dissolved organic matter (DOM) in the aquatic continuum. However, large sample sets are typically needed for establishing a meaningful EEM-PARAFAC model. Applications of the EEM-PARAFAC technique to individual samples require new approaches. Here, flow field-flow fractionation (FlFFF) combined with offline EEM measurements and PARAFAC analysis was used to elucidate the dynamic changes in DOM composition/optical properties with molecular weight within individual samples. FlFFF-derived size spectra of ultrafiltration-isolated colloidal DOM show that peak-C related fluorophores (E_x/E_m= 350/450 nm) are present mostly in the 1−3 kDa size range, while peak-T associated fluorophores (E_x/E_m = 275/340 nm) have a bimodal distribution with peaks in both the 1−3 kDa and the >100 kDa size fractions. The integrated EEM spectra from FlFFF size-fractionated subsamples closely resembled the bulk EEM spectra, attesting to the convincing comparability between bulk and FlFFF size-fractionated EEMs. The PARAFAC-derived DOM components are distinctive among individual samples with the predominant components being humic-like in river water, but protein-like in a highly eutrophic lagoon sample. This compelling new approach combining FlFFF and EEM-PARAFAC can be used to decipher the dynamic changes in size spectra and composition of individual DOM samples from sources to sinks or across the redox/hydrological/trophic interfaces.

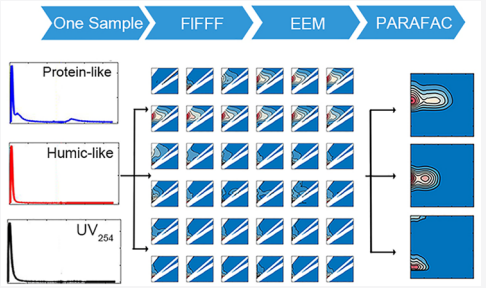

1. INTRODUCTION

Dissolved organic matter (DOM) is ubiquitous and heterogeneous in aquatic environments and plays an essential role in regulating water quality, chemical speciation of many trace elements, and the fate/transport of contaminants.[1−4] Understanding the composition, reactivity, and cycling pathways of DOM is thus indispensable. Previous studies have shown that the bulk DOM contains diverse components with different molecular weights (or sizes), ages, composition/functionalities, and chemical/biological reactivities in natural waters.[5−7] For example, different DOM components within the bulk DOM pool could be preferentially decomposed through different degradation pathways/mechanisms,[8−10] resulting in distinct DOM properties along the aquatic continuum.[11,12] Therefore, size and compositional characterization of individual DOM samples are needed to provide new insights into the lability, transformation, and environmental fate of natural organic matter in the aquatic continuum, especially at the groundwater−surface water, river−lake, and river−sea interfaces.

Due to the small volume requirement and user-friendly analytical procedure, optical properties measured by UV−visible spectroscopy techniques have been widely used in the characterization of DOM in natural waters.[13−17] Furthermore, applications of fluorescence excitation emission matrices (EEM) with parallel factor analysis (PARAFAC) have further enhanced our understanding of the sources, composition, and chemical properties of fluorescent DOM in aquatic environments, especially over the past decade.[18,19] Nevertheless, the EEM-PARAFAC analysis requires a large number of samples to establish statistical models. For individual samples or when the number of samples is limited, new approaches are sorely needed to acquire PARAFAC-derived DOM components.

Natural DOM constantly endures degradation, modification, and transformation during its transport from sources to sinks along the aquatic continuum. As a result, each DOM sample should have its unique molecular size spectrum and distinct DOM composition, especially along stations across river−lake and land−ocean interfaces.[11,12,20,21] Thus, application of the EEM-PARAFAC to the characterization of individual DOM samples is urgently needed to thoroughly decipher dynamic changes in DOM molecular size and size-dependent chemical composition along a specific aquatic continuum.

Flow field-flow fractionation (FlFFF) is an analytical technique capable of simultaneous size separation and

Received: November 24, 2019
Revised: December 24, 2019
Accepted: December 30, 2019
Published: January 2, 2020

chemical characterization of colloidal organic matter, macromolecules, and nanoparticles.[22−24] In the past decades, the FlFFF has been frequently used in aquatic and environmental studies.[21,23,25−27] Recently, Cuss and Guéguen[28] combined the FlFFF with an online fluorescence detector, allowing discrete EEM characterization by halting elution flow.[28] In addition, Zhou and Guo reported the application of FlFFF and offline EEM measurements and showed variations in EEM spectra with selected DOM size fractions in an individual sample.[29] Similarly, Wünsch et al. and Murphy et al. demonstrated their one-sample PARAFAC approach, for the first time, using either high-performance size exclusion chromatography (HPSEC) coupled with an online emission-spectra fluorescence detector through multiple injections or the photochemistry EEM-PARAFAC approach.[30,33] Many previous studies used solid-phase extraction (SPE) and/or XAD resins to preconcentrate DOM for further chemical characterization, which requires the acidification of natural waters to pH < 2 and thus may fractionate DOM compositionally and structurally.[31] In contrast, ultrafiltration-isolated DOM has a well-defined molecular weight range and is based on physical separation without chemical alteration to the DOM.[32] Despite recent progress in DOM characterization and one-sample PARAFAC approach,[30,33,34] combination of FlFFF with offline EEM-PARAFAC analysis has not been reported for single DOM samples, especially for colloidal DOM samples isolated using ultrafiltration.

In this study, a method combining FlFFF separation and characterization with offline EEM measurements was developed to elucidate variations in fluorescence EEM spectra with a molecular weight in individual DOM samples preconcentrated using ultrafiltration with a 1 kDa membrane. Together with PARAFAC analysis on the EEM data from all subsize fractions, major fluorescent DOM components were identified for each individual DOM sample collected from different aquatic environments. Applications of the FlFFF and EEM-PARAFAC to natural DOM samples provide new insights into both size-dependent chemical composition and PARAFAC-derived fluorescent DOM components within individual DOM samples.

2. MATERIALS AND METHODS

2.1. Sample Processing. Three unique water samples were collected from different aquatic environments, including (1) the Milwaukee River, a terrigenous DOM-dominated river in Wisconsin, (2) open Green Bay, a mesotrophic sub-basin of Lake Michigan, and (3) Veterans Lagoon in the City of Milwaukee, a eutrophic lagoon with seasonal algal blooms over the past years. Detailed sampling locations and hydrographic parameters are given in Table 1.

Water samples were collected using acid-cleaned Nalgene bottles. The collected water samples were immediately filtered through precombusted (450 °C for 4 h) GF/F filters (Whatman, 0.7 μm). Aliquots of the <0.7 μm filtrate were sampled for the measurements of dissolved organic carbon (DOC), UV−visible absorption spectrum, and fluorescence EEM.

To optimize the signal-noise ratio for FlFFF fractional samples, an aliquot of the filtrate was preconcentrated using a stirred cell ultrafiltration unit (Amicon 8200) with a 1 kDa membrane (regenerated cellulose, Millipore YM1, 63.5 mm diameter; actually cutoff >1.33 kDa based on an 80−85% rejection rate).[6] Before ultrafiltration, the ultrafiltration disc membrane was precleaned with 0.05 M NaOH solution followed by ultrapure water until the DOM and CDOM signatures were similar to those of ultrapure water.[6] To quantify the abundance of bulk colloidal DOM, time-series permeate samples, in addition to initial, integrated permeate, and retentate samples, were collected for the measurements of CDOM using UV−visible and fluorescence spectrophotometers. The ultrafiltration permeation model was then applied to fit the time-series data to calculate the colloidal DOM abundance,[35] which ranged from 58 to 75% in these three samples (Table 1).

Table 1. Sample Descriptions, Hydrographic Parameters, and Bulk DOM Properties[a]

parameters (unit)	Milwaukee River	Green Bay	Veterans Lagoon
longitude (°W)	−87.910	−87.843	−87.894
latitude (°N)	43.035	44.718	43.046
temperature (°C)	2.4	n/a	15.65
pH	8.28	8.05	8.9
specific conductivity (μS/cm)	882	321	971
DOC (μmol/L)	514	441	413
HMW-DOC (μmol/L)	298	290	309
LMW-DOC (μmol/L)	216	150	106
colloidal DOC (%)	58	66	75
a_{254} (m^{-1})	49.9	27.7	23.2
$S_{275-295}$ (nm^{-1})	0.017	0.020	0.017
$SUVA_{254}$ (L/mg-C/m)	3.51	2.27	2.03
BIX	0.60	0.73	0.71
HIX	4.31	4.82	1.60

[a]Including dissolved organic carbon (DOC), HMW-DOC (>1 kDa), LMW-DOC (a_{254}), a spectral slope between 275 and 295 nm ($S_{275-295}$), specific UV absorbance at 254 nm ($SUVA_{254}$), and fluorescence indices (HIX, humification index, and BIX, biological index) in water samples collected from the lower Milwaukee River, mesotrophic Green Bay/Lake Michigan, and eutrophic Veterans Lagoon/Milwaukee.

2.2. Measurements of DOC and CDOM. Concentrations of DOC were measured using a TOC analyzer (TOC-L, Shimazu).[36] Ultrapure water, working standards, and community-certified DOC samples (from the University of Miami) were measured to monitor the blank level and instrument performance and to ensure data quality.

UV−visible absorption spectra were measured using an Agilent 8453 spectrophotometer.[37] CDOM absorption coefficients at 254 nm (a_{254}) were calculated using the following equation: a_{254} (m^{-1}) = 2.303 × A(254 nm)/l, where a_{254} is the Naperian absorption coefficient at 254 nm, A(254 nm) is the absorbance at 254 nm, and l is the path length of the cuvette (in meters). Spectral slopes between 275 and 295 nm ($S_{275-295}$ in nm^{-1}) were calculated using the following equation: $a_\lambda = a_{\lambda_0} e^{-S_{275-295}(\lambda-\lambda_0)}$. Linear regression was performed to fit the absorption spectra to the log-transformed equation: $\ln a_\lambda = \ln a_{\lambda_0} - S_{275-295}(\lambda - \lambda_0)$.[38] $SUVA_{254}$, an indicator of aromaticity, was calculated as: $SUVA_{254} = A(254\ nm)/DOC$, with a dimension of L/m/mg-C.

2.3. Separation and Characterization of DOM using FlFFF. The FlFFF system (AF2000, Postnova), equipped with a 0.3 kDa polyether sulfone ultrafiltration membrane (with an actual cutoff of >1 kDa based on a 90% rejection rate),[29] is coupled online with a UV-absorbance detector and two

https://dx.doi.org/10.1021/acs.est.9b07123
Environ. Sci. Technol. XXXX, XXX, XXX−XXX

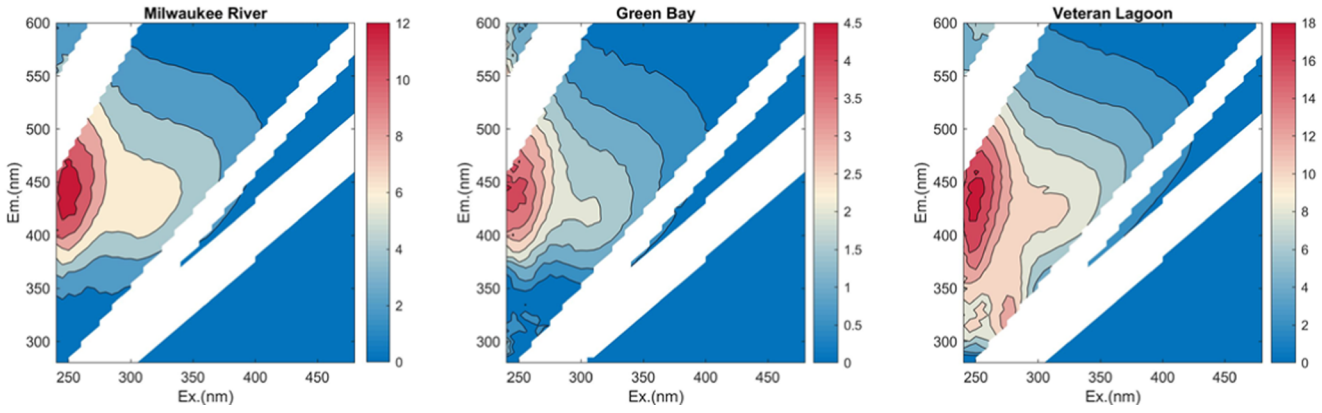

Figure 1. Excitation−emission matrix (EEM) spectra of the bulk water samples from the Milwaukee River (left), Green Bay (middle), and Veterans Lagoon (right).

fluorescence detectors. Carrier solution was prepared from 10 mmol/L NaCl (aq) and 5 mmol/L H_3BO_3 (aq) and pH of 8 (adjusted with NaOH) for optimal separation. Calibrations of DOM molecular size (in kDa or nm) against elution time have been described elsewhere.[25,29]

Flow settings (including tip flow, focus flow, cross flow, etc.) followed those in previous studies.[29] Briefly, the focus flow was 2.1 mL/min, while the tip flow was 0.1 mL/min. The resultant high ratio of the focus to the tip flow rate guaranteed an optimal preseparation condition. The cross flow rate was set at 1.5 mL/min. After 15 min of focusing, cross flow and outlet flow remained constant at 1.5 and 0.7 mL/min, respectively. At the same time, the tip flow increased to 2.2 mL/min, and the focus flow gradually declined to zero, shifting the FlFFF status from focusing to eluting. The eluting lasted 20 min to thoroughly separate colloidal DOM molecules in the channel. After eluting, cross flow linearly declined to zero, while the tip flow linearly declined from 2.2 to 0.7 mL/min. In this 15 min step, the flow field produced by cross flow gradually decreased to zero, which flushed out large molecules retaining above the membrane.

Online DOM characterization was conducted using a UV-absorbance detector (SPD-20A, Shimazu) and two fluorescence detectors (RF-20A, Shimadzu) with different excitation/emission (E_x/E_m) combinations. Absorbance at 254 nm (UV_{254}) is commonly regarded as an indicator of CDOM abundance in natural waters.[14,39] Thus, UV absorbance at 254 nm was selected to monitor changes in bulk CDOM along its colloidal size continuum within each sample. The fluorescence detectors were used to measure the UVC humic-like fluorophores, also known as peak C (E_x/E_m at 350/450 nm), and the tryptophan- or protein-like fluorophores, also known as peak T (E_x/E_m at 275/340 nm). All signatures are expressed in the quinine sulfate equivalent unit (ppb-QSE).

The FlFFF-derived size-fractionated subsamples were collected for offline fluorescence EEM measurements using 5 mL precombusted glass vials. To optimize both size resolution and EEM analysis, size-fractioned subsamples were collected at either 1 or half-minute time interval during elution depending on the distribution of major peaks and fractograms. To balance size spectrum resolution and subsamples' fluorescence signal intensity, multiple injections (3 for the 1 min subsamples and 7 for the half-minute subsamples) are needed depending on DOM abundances. In general, ≥40 subsamples were collected from each sample for offline EEM measurements. To eliminate the systematical EEM blanks from FlFFF, the carrier solution was run as a sample on the same FlFFF system, and all size-fractionated carrier subsamples were collected for EEM measurements. Each corresponding background EEM signal was then subtracted from sample's EEM spectra.

2.4. Measurements of EEM Spectra and PARAFAC Analysis. Fluorescence EEM spectra of FlFFF-fractionated DOM subsamples were measured using a Fluoromax-4 spectrofluorometer (Horiba Jobin Yvon).[40] Excitation wavelength was set in the range from 250 to 450 nm with 5 nm intervals, and emission wavelengths varied from 220 to 600 nm with 5 nm intervals. Ultrapure water was referenced to eliminate background noise for the bulk samples. For the size-fractionated subsamples, the FlFFF size-fractionated carrier solution samples were used as their EEM blanks. To eliminate inner filter effects, samples were diluted to absorbance values at 254 nm <0.02 before EEM measurements. Electric signals of emission and excitation spectra were corrected, normalized, and calibrated to QSE.[41] First and second orders of Raman and Rayleigh scattering peaks were eliminated. The biological index (BIX) is the ratio of fluorescence intensity at 380−430 nm within an excitation wavelength of 310 nm.[42] The humification index (HIX) is the ratio of fluorescence signals at the range of 435−480 nm to those at the range of 300−345 nm overexcitation at 254 nm.[43]

PARAFAC analysis was performed on the EEM data acquired from all FlFFF-fractionated samples. The model was constrained to non-negative values, and the results were validated using split-half analysis.[18,19] All data handling and analysis described above were performed in MATLAB 2017a (MathWorks) using the drEEM toolbox.[44] Detailed comparison and validation for the PARAFAC model using Tucker's congruence coefficient (TCC) and PARAFAC model parameters are given in the Supporting Information (SI Sections 1 and 2).

3. RESULTS AND DISCUSSION

3.1. Bulk DOM Properties. Before further size fractionation and FlFFF analysis, water samples were characterized for the bulk properties including DOC concentration, absorption coefficient (a_{254} or CDOM), EEM spectra, and other optical properties, such as $SUVA_{254}$, spectral slope, and fluorescence indices, including HIX and BIX (Table 1 and Figure 1).

For the Milwaukee River sample, bulk DOC concentration was 514 μM, and a_{254} value was 49.9 m^{-1}, both of which are

https://dx.doi.org/10.1021/acs.est.9b07123
Environ. Sci. Technol. XXXX, XXX, XXX−XXX

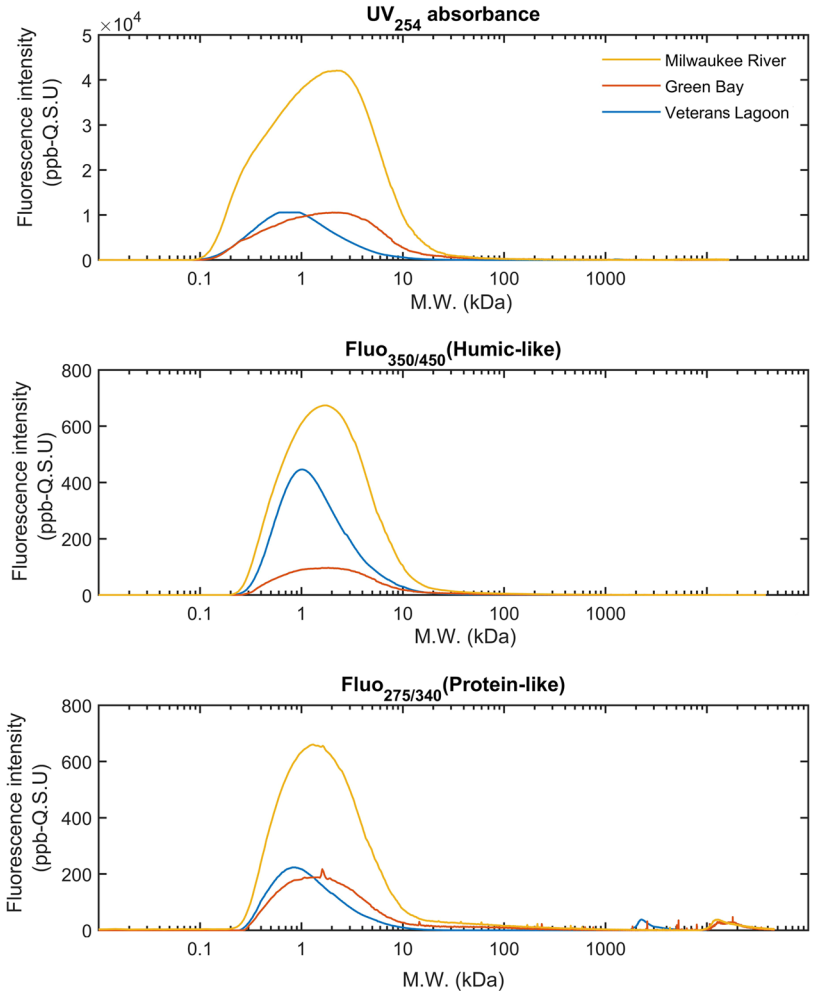

Figure 2. FlFFF fractograms of the three colloidal DOM samples, including UV absorbance at 254 nm (top), fluorescent humic-like at E_x/E_m = 350/450 nm (middle), and fluorescent protein-like at E_x/E_m = 275/340 nm (bottom). Notice that a log-scale was used here for the *x*-axis or molecular weight (MW).

within the ranges of major US rivers[39] and Wisconsin rivers.[37,45] Values of $SUVA_{254}$ (3.51 L/mgC/m) and the spectral slope ($S_{275-295}$ = 0.0170 nm^{-1}) were almost the same as those in the Fox River/Milwaukee River (3.01/3.60 L/mgC/m; 0.0197/0.0170 nm^{-1}, respectively)[37,45] although $SUVA_{254}$ was relatively higher than the lower Mississippi River and some other US rivers,[39,46] indicating higher aromaticity and prevailed vascular plant input in the water sample.[16,38] In terms of colloidal organic carbon abundance, 58% of the bulk DOC was measured in the >1 kDa colloidal fraction and the remaining 42% was partitioned in the <1 kDa low-molecular-weight (LMW) fraction (Table 1), similar to those found in other river waters.[32]

For the mesoeutrophic Green Bay sample, both DOC concentration and a_{254} were in the ranges reported previously,[12] but significantly lower than those of the Milwaukee River sample (Table 1). Similar to other areas,[35] the $S_{275-295}$ value was slightly higher than those in river waters, indicating a relatively low in CDOM molecular weight. The colloidal DOC abundance in the Green Bay water sample was relatively high compared to that in Milwaukee River water, with 66% of DOC measured in the >1 kDa colloidal or HMW-DOM fraction (Table 1). For the Veterans Lagoon sample, the DOC concentration and a_{254} were relatively low compared to the other two samples. However, up to 75% of DOC was measured in the >1 kDa colloidal phase in this eutrophic water sample (Table 1), likely derived from algal exudates or degradation products.

The fluorescence EEM spectra of the three bulk water samples are depicted in Figure 1. The EEM contours of the Milwaukee River and Green Bay samples are similar, showing two obvious peaks, peak A (E_x/E_m = 260/400−460 nm) and peak C (E_x/E_m = 320−360/420−460 nm), which are related to humic-like fluorophores.[15,16] The predominance of terrestrial humic-like DOM in the Milwaukee River sample is consistent with previous observations in the same river.[45] The EEM contour of the eutrophic lagoon sample was distinct from the other two samples (Figure 1). In addition to peaks A and C in the sample, peak T (E_x/E_m = 275/340 nm) was another major peak, indicating a significant contribution of autochthonous DOM to the eutrophic lagoon sample.

Fluorescence indices (BIX and HIX) derived from EEM data have been used to explore potential DOM sources that might be ignored using the empirical peak-based method.[33,42,43,47] A HIX < 4 can be regarded as the DOM source with scarce humic materials, while a BIX of 0.6−0.7 is related to the DOM source with a mediocre level of autochthonous materials.[42] As shown in Table 1, the value of HIX was 4.31 in the river water sample and 4.82 in the Green Bay water, which are similar to those previously observed in the Milwaukee

https://dx.doi.org/10.1021/acs.est.9b07123
Environ. Sci. Technol. XXXX, XXX, XXX−XXX

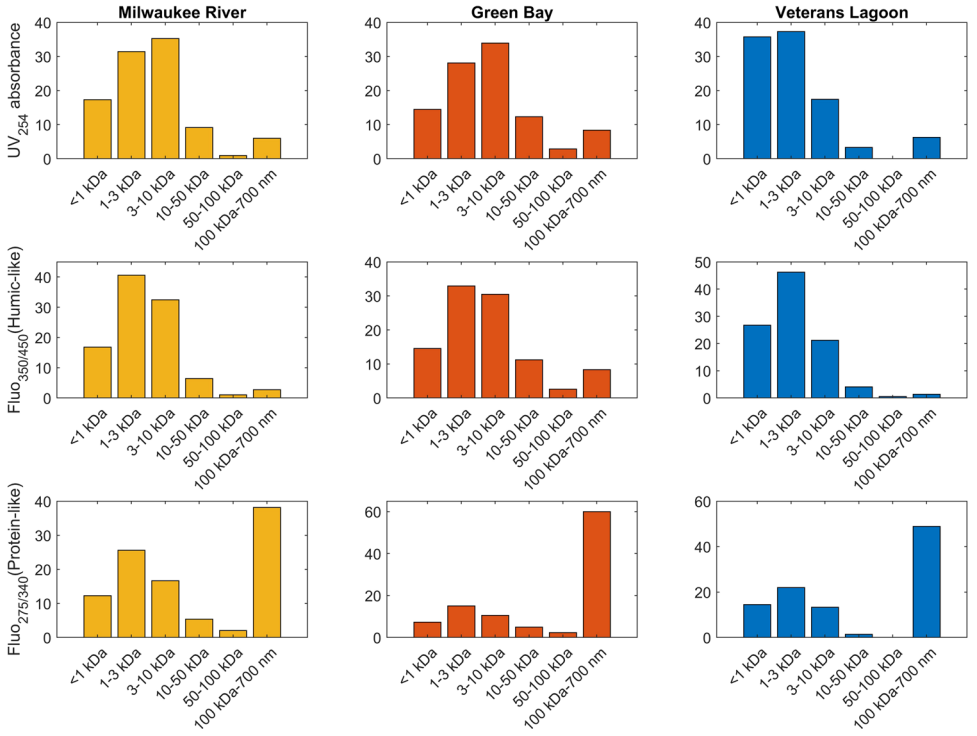

Figure 3. Size distributions of optical properties among the integrated size intervals in samples collected from the Milwaukee River (left), Green Bay (middle), and Veterans Lagoon (right), including UV absorbance at 254 nm (top), fluorescent humic-like at E_x/E_m = 350/450 nm (middle), and fluorescent protein-like at E_x/E_m = 275/340 nm (bottom). The seemingly difference in the distribution of larger size classes between the continuous fractograms (log-scaled, Figure 2) and the integrated fractograms (linear scale, this figure) was largely due to the shrinking of signals in the size fractions >10 kDa.

River,[45] the Fox River, and Green Bay,[37] but higher than the HIX value measured for the Veterans Lagoon sample and those reported previously for the oligotrophic Great Lakes.[40] The value of BIX was 0.60 for the river water sample, which is slightly lower than those measured for the Green Bay and Veterans Lagoon samples (Table 1) or the Great Lakes,[40] but similar to those measured for the Milwaukee River[45] and the Fox River.[37] Intermediate HIX and BIX values in the river and bay waters suggested a mixed DOM pool from both prevailed humic-like materials and autochthonous components derived from microbial transformation, while low HIX value in the eutrophic lagoon sample pointed to a predominant autochthonous DOM source.

3.2. Continuous Size Distribution of Colloidal DOM Characterized using FlFFF. The FlFFF technique is capable of simultaneous size separation and characterization depending on detectors. Fractograms derived from the FlFFF analysis are shown in Figure 2. Colloidal DOM in the river water had high UV_{254} absorbance and fluorescence intensities (both humic-like and protein-like) due to its higher DOC concentration and $SUVA_{254}$ value compared to the other two samples. The UV_{254}-absorbance and both humic-like and protein-like fluorescent components (denoted by $Fluo_{350/450}$ and $Fluo_{275/345}$, respectively) have a major peak in the <10 kDa size range. In addition, there existed a secondary peak for protein-like fluorophores at the >100 kDa (Figures 2 and 3). Although similar fractograms are observed among these three samples, their specific peak locations and intensities in UV_{254} absorbances and fluorescent components are clearly different (Figure 2).

When the continuous fractograms (Figure 2 with log-scaled molecular weight) were integrated and then divided into selected size classes, e.g., the <1, 1−3, 3−10, 10−50, 50−100, and >100 kDa (Figure 3), the percentages of each size class in the total integrated signal could be calculated. For example, UV_{254} absorbance was highest in the 3−10 kDa size range for the river and bay water samples and in the 1−3 kDa size range for the eutrophic lagoon sample (Figure 3). Similarly, peak C-related fluorophores or humic-like substances (i.e., $Fluo_{350/450}$) were mostly partitioned in the 1−3 kDa size range for all three samples followed by the 3−10 kDa and the <1 kDa size fractions, with the >10 kDa size fractions being the least (Figure 3). For peak T-related fluorophores or protein-like substances (i.e., $Fluo_{275/340}$), however, the major molecular size fraction was the >100 kDa or the 100 kDa−700 nm in all three samples, followed by the 1−3 and 3−10 or <1 kDa size fractions (Figure 3). For both humic-like and protein-like substances, the intensities of different DOM size fractions consistently decreased with increasing molecular weight within the size range between 1 and 100 kDa, although there is a significant difference in the continuous molecular size distribution between humic-like and protein-like substances (Figure 3). The seemingly difference in the DOM size distribution between the log-scaled fractograms (Figure 2) and the integrated size classes (Figure 3) is largely due to the amplification of signals of the lower molecular size range (~1 kDa) and compression of those in the >10 kDa size fraction (Figure 2). Similar DOM size distributions derived from FlFFF analysis have also been observed in other aquatic environments.[21,24]

Overall, the humic-like substances (E_x/E_m at 350/450 nm) are mostly partitioned in the 1−3 kDa size range, while the protein-like substances (E_x/E_m at 275/340 nm) are largely

https://dx.doi.org/10.1021/acs.est.9b07123
Environ. Sci. Technol. XXXX, XXX, XXX−XXX

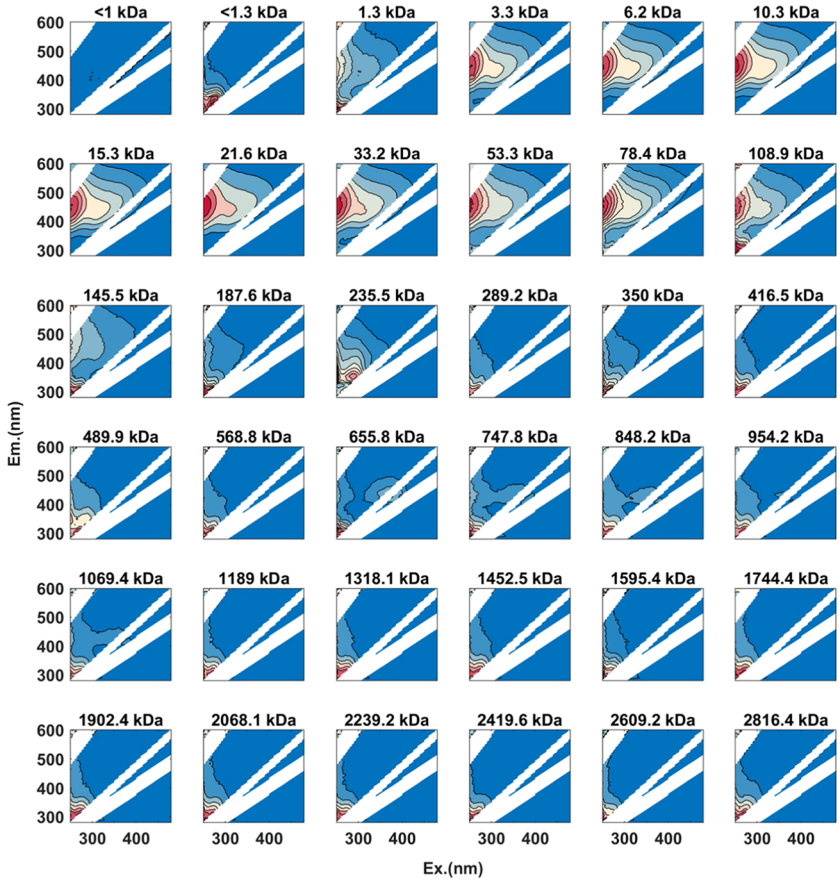

Figure 4. Examples of EEM spectra in FlFFF-generated size fractions along the size continuum, showing dynamic changes in the fluorescence EEM characteristics with molecular weight within the individual DOM sample from the Milwaukee River.

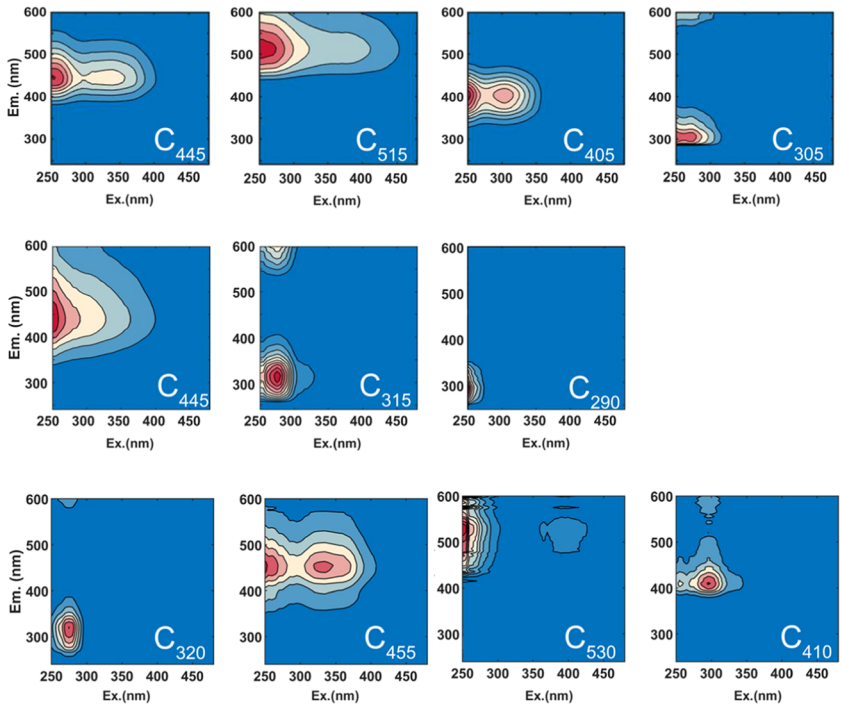

Figure 5. Contour plots showing distinctive PARAFAC-derived major fluorescent DOM components for three different water samples from the Milwaukee River (top), Green Bay (middle), and Veterans Lagoon (bottom) using FlFFF and EEM-PARAFAC analysis (see Table 2 for the characteristic E_x/E_m wavelengths of each DOM component).

https://dx.doi.org/10.1021/acs.est.9b07123
Environ. Sci. Technol. XXXX, XXX, XXX−XXX

present in the >100 kDa size fraction with a bimodal distribution with a second peak at the 1−3 kDa size fraction.

3.3. Molecular Size-Dependent EEM Spectra. As shown in Figure 2, the FlFFF technique coupled with online detectors provides a continuous size distribution of bulk DOM. Offline measurements on the FlFFF size-fractionated subsamples using three-dimensional (3D) spectrofluorometer, on the other hand, offer EEM spectra of different DOM molecular size fractions in the same sample, revealing continuous changes in fluorescence EEM characterization from small-molecular-weight to large-molecular-weight (>100 kDa) fractions within individual samples (Figure 4).

Examples showing the application of FlFFF combined with offline EEM measurements and changes in EEM spectra with DOM molecular weight in the river water sample are given in Figure 4. Indeed, the results demonstrated clearly a change in fluorescence EEM characteristics with increasing DOM molecular size within the specific individual water sample (Figure 4). For example, the fluorophores characterized with peaks A and C were dominantly present in the molecular size fractions between 3 and 100 kDa, and then faded away gradually with increasing size. Peak M (E_x/E_m = 290−310/370−410 nm) appeared between ~650 and 850 kDa although somewhat weak. A part of the peak was masked by the first-order Rayleigh and Raman scattering peaks of water, making it difficult to be identified. Its intensity was relatively low compared with peak B (E_x/E_m = 275/305 nm).

Fluorophores associated with peak B appeared mostly in the >78 kDa. Intriguingly, the humic-like substances, including peaks A and C,[13,15,29] were largely partitioned in the lower MW size fractions (<100 kDa), while the protein-like substances, such as peaks B and T, were present in the higher MW DOM fractions (>78 kDa). These unique size distributions between humic-like and protein-like DOM, revealed by the FlFFF-EEM technique, are consistent with their characteristics in molecular size, surface-reactivity (such as dispersiveness, aggregation, and self-assembly), and environmental behavior.[3,9,48,49] For example, humic substances have been shown to be detergent-type highly dispersive organic matter,[48] while proteins can be formed from aggregation of amino acids and peptides and contain mostly HMW materials.[49] Thus, the application of FlFFF-EEM and the resultant molecular size-dependent EEM spectra in individual bulk DOM samples as exemplified in Figure 4 allow the identification of not only the variation in the relative importance of different fluorescent components with molecular weight but also the less visible minor fluorophores in the bulk EEM spectra.

3.4. PARAFAC-Derived DOM Components for Individual Samples. PARAFAC analysis was performed for each water sample based on the EEM data of FlFFF-derived size-fractionated samples, resulting in three different models that were validated by half-split analysis. Figure S1 (SI Section 2) shows the sum of squared error from excitation and emission spectra for each sample. As shown in Figure 5, four different fluorescent DOM components were identified for the river water and the eutrophic lagoon water, but only three fluorescent components were identified for the mesotrophic bay water, demonstrating different major fluorescent DOM components among the three water samples.

Within the four components in the river water sample, three (C1, C2, and C3 or C_{445}, C_{515}, and C_{405}) are humic-like materials with their E_x/E_m maxima at 255/445, 250/515, and 250/405 nm, respectively. They are related to peaks A and C.[15,41] These three terrestrially derived DOM components have been widely observed in aquatic environments.[37,40,50,51] The fourth component (C4 or C_{305}) is identified as protein-like materials with the E_x/E_m centered at 250/305 nm (Table 2), which is empirically regarded as the combination of peaks B and T from autochthonous sources.[15] However, it has the least contribution (15.9%) compared to those humic-like components, which contributed up to 84.1% of the total fluorescence intensity (Table 2). Within the three fluorescent components in the mesotrophic bay water, the predominant component is the UVC humic-like materials mainly from the terrestrial input.[52] The other two are tryptophan-like and tyrosine-like components, which are typical protein-like materials in natural waters (Figure 5 and Table 2). For the eutrophic lagoon water sample, protein-like component (E_x/E_m = 275/320 nm), contributing 28.2% of the total fluorescence, is the dominant component related to tyrosine-like (E_x/E_m = 275/305 nm) and tryptophan-like (E_x/E_m = 275/340 nm) components. The other three fluorescent components are humic-like components (Figure 5 and Table 2).

Table 2. PARFAC-Derived Major Fluorescent DOM Components for Each Sample and Their Relative Contributions to the Total Fluorescence within Individual Water Samples

components	E_x (nm)	E_m (nm)	description	contribution (%)
Sample from the Milwaukee River				
C1 (C_{445})	255	445	humic-like	34.9
C2 (C_{515})	250	515	humic-like	23.9
C3 (C_{405})	250	405	humic-like	25.2
C4 (C_{305})	250	305	protein-like (tryptophan-like)	15.9
Sample from Green Bay				
C1 (C_{445})	250	445	humic-like	44.1
C2 (C_{315})	275	315	protein-like (tryptophan-like)	31.9
C3 (C_{290})	250	290	protein-like	24.0
Sample from Veterans Lagoon				
C1 (C_{320})	275	320	protein-like (tryptophan-like)	28.2
C2 (C_{455})	250/335	455	humic-like	28.4
C3 (C_{530})	250/390	530	humic-like	19.0
C4 (C_{410})	295	410	humic-like	24.4

Quantitative comparisons in the PARAFAC-derived components between the three samples using the TCC method (Tables S1−S3) show that only the C_{445} fluorescent component was found common in all three samples (with TCC_{E_x/E_m} values >0.90) although all of the PARAFAC-derived fluorescent components have been reported previously.[15,30,34,53] This again manifests the uniqueness in major DOM components among samples collected from different aquatic environments. When the E_x/E_m loadings from these components were uploaded for online comparisons using the OpenFluor database[54] and when the thresholds for the E_x/E_m minimum similarity scores were set at 0.95, the loadings of C1, C2, C3, and C4 (or C_{445}, C_{515}, C_{405}, and C_{305}) from the Milwaukee River sample match components in 40, 34, 37, and 6 cases/datasets, respectively. In addition, comparing compo-

https://dx.doi.org/10.1021/acs.est.9b07123
Environ. Sci. Technol. XXXX, XXX, XXX−XXX

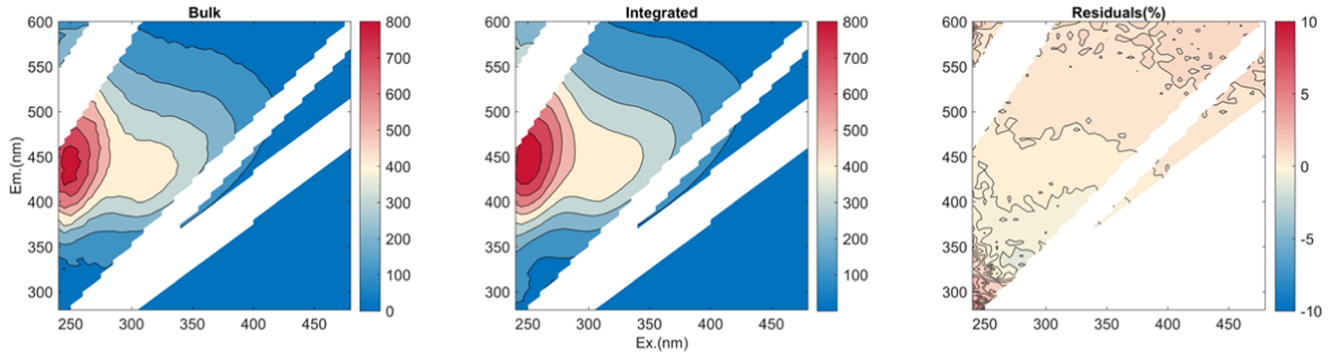

Figure 6. EEM spectra of the bulk water sample (left panel) and the integrated subsamples (middle panel) for the Milwaukee River sample and a mass balance or EEM residuals (right panel) between the bulk and the integrated subsamples.

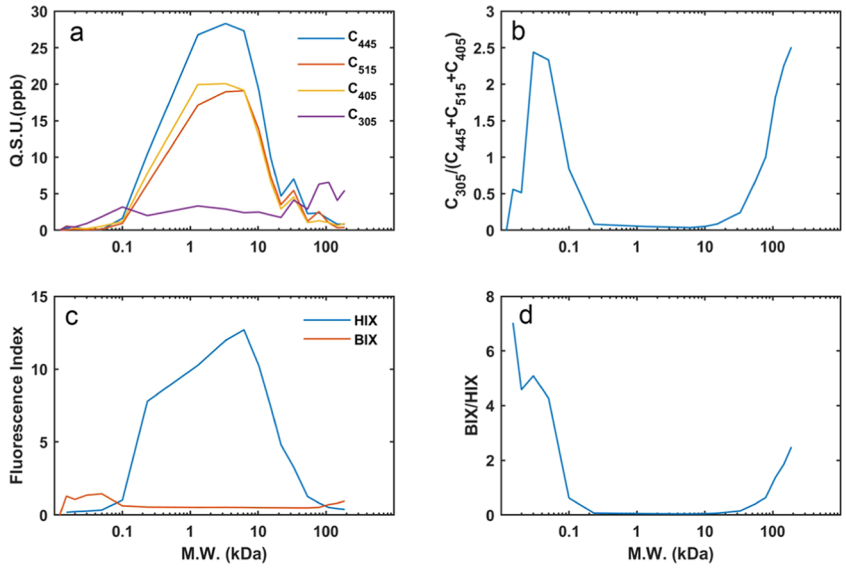

Figure 7. Variations in the four PARAFAC-derived fluorescent components (a), fluorescence intensity ratio of C_{305} to (C_{445} + C_{515} + C_{405}), an indicator for the relative contribution of protein-like substances (b), fluorescence indices (HIX and BIX) (c), and the BIX/HIX ratio (d) with molecular weight (MW) within the Milwaukee River water sample (see also Figure S4 for changes in the distribution of PARAFAC-derived fluorescent components with molecular weight).

nents C_{445}, C_{515}, C_{405}, and C_{305} identified for the Milwaukee River with those (F_{400}, F_{420}, F_{450}, and F_{520}) reported in Murphy et al.,[34] three out of the four components (i.e., C_{445}, C_{515}, and C_{405}) are highly congruence with their F_{450}, F_{520}, and F_{400}, respectively (TCC_{E_x/E_m} > 0.95). These three humic-like components (C_{445}, C_{515}, and C_{405}) are also highly similar to those derived from the HPSEC-EEM-PARAFAC method for the Rio Negro sample[30] (TCC_{E_x/E_m} > 0.95). Fewer cases reported the same protein-like component (C4 or C_{305} here), probably due to the low signal/noise ratio in the UV-A area and sample's unique DOM regime under different hydrological and/or trophic conditions.

To further validate the new approach, the "mass balance" of fluorophores between the bulk and subfractional samples was evaluated using comparisons between the integrated EEM spectra from all subsamples and the EEM spectra from the bulk water sample. As shown in Figure 6 for the Milwaukee River sample, the integrated EEM and the bulk EEM spectra resemble each other in both fluorescence intensity and spectral characteristics. Fluorescence intensities of major peaks (peaks A, C, and M) recovered from all subsamples comprised up to 98.4, 99.5, and 99.8%, respectively, of their corresponding intensities in the bulk sample (Table S4). Differences between the integrated EEM and the original EEM spectra are reflected in the residuals given in Figure 6. In the major peaks areas (i.e., Peaks C and A; E_m > 400 nm), the residuals are negligible since their fluorescence signals are high and the spectral corrections are reliable. Outside the major peaks in the EEM spectra, some residuals are visible due to their low intensities, but they are all within ±10% and mostly observed in the UV-A area (E_m < 400 nm, Figure 6). Negative residuals in E_m at 320−400 nm area are probably related to the loss of DOM through sorption onto the FlFFF system (e.g., tubing and membrane). On the other hand, positive residuals below the 320 nm likely result from the low signal/noise ratio in the specific wavelength region. Overall, the spectra of the integrated EEM from size-fractionated subsamples and the bulk EEM spectra from the original sample closely resemble each other and the residuals are in general negligible, attesting to the applicability and validity of the approach combining FlFFF and EEM-PARAFAC.

3.5. Changes in DOM Properties with Molecular Weight within Individual Samples. As shown in Figure 7, the three humic-like components (C_{445}, C_{515}, and C_{405}) all presented mostly in the <20 kDa size range, with a minor peak

https://dx.doi.org/10.1021/acs.est.9b07123
Environ. Sci. Technol. XXXX, XXX, XXX−XXX

in the 25−45 kDa and negligible in the >45 kDa. For the protein-like component (C_{305}), its relative abundance increased in general with MW, with peaks mostly between ∼30 and >100 kDa. High protein-like to humic-like ratio (i.e., $C_{305}/(C_{445} + C_{515} + C_{405})$) was found in the <0.3 and >20 kDa size ranges, indicating that protein-like DOM was present mainly in either lower MW < 0.3 kDa or higher MW > 20 kDa, especially the >100 kDa size fraction. In contrast, humic-like components occurred preferentially in the 0.3−20 kDa size range.

Similarly, fluorescence indices also demonstrated a dynamic variation with molecular weight within the sample (Figure 7c,d), showing that high humified DOM components had a MW of ∼6 kDa and elevated BIX occurred in the <0.3 and >100 kDa size ranges. This bimodal distribution of BIX resembled those of protein-like components and the $C_{305}/(C_{445} + C_{515} + C_{405})$ ratio (Figure 7b). Similar results are shown for the other samples in the SI (Figures S2 and S3).

These detailed features showing dynamic changes in the size-dependent distribution of optical properties and PARAFAC-derived DOM components within an individual sample could not have been revealed by the EEM spectra of bulk samples. Therefore, the combination of FlFFF size fractionation and EEM-PARAFAC analysis provides a compelling approach to the characterization of DOM composition and molecular size spectra for individual samples. When applied to samples along the aquatic continuum, they will provide new insights into the source, environmental fate, mixing behavior, and cycling pathways of DOM, especially at the groundwater−surface water, river−lake, and land−ocean interfaces.

■ ASSOCIATED CONTENT

Supporting Information

The Supporting Information is available free of charge at https://pubs.acs.org/doi/10.1021/acs.est.9b07123.

Comparison between components; PARAFAC model statistic details; Tucker's congruence coefficient (TCC) of emission spectra and excitation spectra between Milwaukee Rive and Green Bay samples; comparisons in the fluorescence intensities of peaks A, C, and M in the EEM spectra between the bulk sample and those recovered from the integrated FlFFF size-fractionated subsamples for the DOM in samples (PDF)

■ AUTHOR INFORMATION

Corresponding Author

Laodong Guo − *University of Wisconsin-Milwaukee, Milwaukee, Wisconsin;* orcid.org/0000-0002-5010-1630; Email: guol@uwm.edu

Other Author

Hui Lin − *University of Wisconsin-Milwaukee, Milwaukee, Wisconsin*

Complete contact information is available at: https://pubs.acs.org/10.1021/acs.est.9b07123

Notes

The authors declare no competing financial interest.

■ ACKNOWLEDGMENTS

We thank Bin Yang, Dan Li, Dongxu Zhang, Sarah Bartlett, and Wilson Tarpey for their assistance during sample collection and processing and three anonymous reviewers for their constructive comments and valuable suggestions, which greatly improved the manuscript. We acknowledge the support from China Scholarship Council (#201606310069), the University of Wisconsin−Milwaukee, and the UWM's Distinguished Graduate Student Fellowship (to H.L.).

■ REFERENCES

(1) Aiken, G. R.; Hsu-Kim, H.; Ryan, J. N. Influence of Dissolved Organic Matter on the Environmental Fate of Metals, Nanoparticles, and Colloids. *Environ. Sci. Technol.* **2011**, *45*, 3196−3201.

(2) Kim, J.; Kim, G. Inputs of Humic Fluorescent Dissolved Organic Matter via Submarine Groundwater Discharge to Coastal Waters off a Volcanic Island (Jeju, Korea). *Sci. Rep.* **2017**, *7*, No. 7921.

(3) Kteeba, S. M.; El-Adawi, H. I.; El-Rayis, O. A.; El-Ghobashy, A. E.; Schuld, J. L.; Svoboda, K. R.; Guo, L. Zinc Oxide Nanoparticle Toxicity in Embryonic Zebrafish: Mitigation with Different Natural Organic Matter. *Environ. Pollut.* **2017**, *230*, 1125−1140.

(4) Philippe, A.; Schaumann, G. E. Interactions of Dissolved Organic Matter with Natural and Engineered Inorganic Colloids: A Review. *Environ. Sci. Technol.* **2014**, *48*, 8946−8962.

(5) Benner, R.; Amon, R. M. W. The Size-Reactivity Continuum of Major Bioelements in the Ocean. *Annu. Rev. Mar. Sci.* **2015**, *7*, 185−205.

(6) Xu, H.; Guo, L. Molecular Size-Dependent Abundance and Composition of Dissolved Organic Matter in River, Lake and Sea Waters. *Water Res.* **2017**, *117*, 115−126.

(7) Xu, H.; Guan, D.-X.; Zou, L.; Lin, H.; Guo, L. Contrasting Effects of Photochemical and Microbial Degradation on Cu(II) Binding with Fluorescent DOM from Different Origins. *Environ. Pollut.* **2018**, *239*, 205−214.

(8) Hansen, A. M.; Kraus, T. E. C.; Pellerin, B. A.; Fleck, J. A.; Downing, B. D.; Bergamaschi, B. A. Optical Properties of Dissolved Organic Matter (DOM): Effects of Biological and Photolytic Degradation. *Limnol. Oceanogr.* **2016**, *61*, 1015−1032.

(9) Xu, H.; Guo, L. Intriguing Changes in Molecular Size and Composition of Dissolved Organic Matter Induced by Microbial Degradation and Self-Assembly. *Water Res.* **2018**, *135*, 187−194.

(10) Chen, M.; Jaffé, R. Quantitative Assessment of Photo- and Bio-Reactivity of Chromophoric and Fluorescent Dissolved Organic Matter from Biomass and Soil Leachates and from Surface Waters in a Subtropical Wetland. *Biogeochemistry* **2016**, *129*, 273−289.

(11) Abdulla, H. A. N.; Minor, E. C.; Dias, R. F.; Hatcher, P. G. Transformations of the Chemical Compositions of High Molecular Weight DOM along a Salinity Transect: Using Two Dimensional Correlation Spectroscopy and Principal Component Analysis Approaches. *Geochim. Cosmochim. Acta* **2013**, *118*, 231−246.

(12) Xu, H.; Houghton, E. M.; Houghton, C. J.; Guo, L. Variations in Size and Composition of Colloidal Organic Matter in a Negative Freshwater Estuary. *Sci. Total Environ.* **2018**, *615*, 931−941.

(13) Mcknight, D. M.; Boyer, E. W.; Westerhoff, P. K.; Doran, P. T.; Kulbe, T.; Andersen, D. T. Spectrofluorometric Characterization of Dissolved Organic Matter for Indication of Precursor Organic Material and Aromaticity. *Limnol. Oceanogr.* **2001**, *46*, 38−48.

(14) Weishaar, J. L.; Aiken, G. R.; Bergamaschi, B. A.; Fram, M. S.; Fujii, R.; Mopper, K. Evaluation of Specific Ultraviolet Absorbance as an Indicator of the Chemical Composition and Reactivity of Dissolved Organic Carbon. *Environ. Sci. Technol.* **2003**, *37*, 4702−4708.

(15) Coble, P. G. Marine Optical Biogeochemistry: The Chemistry of Ocean Color. *Chem. Rev.* **2007**, *107*, 402−418.

(16) Murphy, K. R.; Butler, K. D.; Spencer, R. G. M.; Stedmon, C. A.; Boehme, J. R.; Aiken, G. R. Measurement of Dissolved Organic Matter Fluorescence in Aquatic Environments: An Interlaboratory Comparison. *Environ. Sci. Technol.* **2010**, *44*, 9405−9412.

(17) Osburn, C. L.; Handsel, L. T.; Mikan, M. P.; Paerl, H. W.; Montgomery, M. T. Fluorescence Tracking of Dissolved and

Particulate Organic Matter Quality in a River-Dominated Estuary. *Environ. Sci. Technol.* **2012**, *46*, 8628−8636.
(18) Stedmon, C. A.; Markager, S.; Bro, R. Tracing Dissolved Organic Matter in Aquatic Environments Using a New Approach to Fluorescence Spectroscopy. *Mar. Chem.* **2003**, *82*, 239−254.
(19) Stedmon, C. A.; Bro, R. Characterizing Dissolved Organic Matter Fluorescence with Parallel Factor Analysis: A Tutorial. *Limnol. Oceanogr. Methods* **2008**, *6*, 572−579.
(20) Abdulla, H. A. N.; Minor, E. C.; Hatcher, P. G. Using Two-Dimensional Correlations of 13 C NMR and FTIR To Investigate Changes in the Chemical Composition of Dissolved Organic Matter along an Estuarine Transect. *Environ. Sci. Technol.* **2010**, *44*, 8044−8049.
(21) Zhou, Z.; Stolpe, B.; Guo, L.; Shiller, A. M. Colloidal Size Spectra, Composition and Estuarine Mixing Behavior of DOM in River and Estuarine Waters of the Northern Gulf of Mexico. *Geochim. Cosmochim. Acta* **2016**, *181*, 1−17.
(22) Giddings, J. C. Field-Flow Fractionation : Analysis of Macromolecular, Colloidal, and Particulate Materials. *Science* **1993**, *260*, 1456−1465.
(23) Baalousha, M.; Stolpe, B.; Lead, J. R. Flow Field-Flow Fractionation for the Analysis and Characterization of Natural Colloids and Manufactured Nanoparticles in Environmental Systems: A Critical Review. *J. Chromatogr. A* **2011**, *1218*, 4078−4103.
(24) Stolpe, B.; Guo, L.; Shiller, A. M. Binding and Transport of Rare Earth Elements by Organic and Iron-Rich Nanocolloids in Alaskan Rivers, as Revealed by Field-Flow Fractionation and ICP-MS. *Geochim. Cosmochim. Acta* **2013**, *106*, 446−462.
(25) Stolpe, B.; Guo, L.; Shiller, A. M.; Hassellöv, M. Size and Composition of Colloidal Organic Matter and Trace Elements in the Mississippi River, Pearl River and the Northern Gulf of Mexico, as Characterized by Flow Field-Flow Fractionation. *Mar. Chem.* **2010**, *118*, 119−128.
(26) Cuss, C. W.; Guéguen, C. Distinguishing Dissolved Organic Matter at Its Origin: Size and Optical Properties of Leaf-Litter Leachates. *Chemosphere* **2013**, *92*, 1483−1489.
(27) Lin, H.; Chen, M.; Zeng, J.; Li, Q.; Jia, R.; Sun, X.; Zheng, M.; Qiu, Y. Size Characteristics of Chromophoric Dissolved Organic Matter in the Chukchi Sea. *J. Geophys. Res.: Oceans* **2016**, *121*, 6403−6417.
(28) Cuss, C. W.; Gueguen, C. Determination of Relative Molecular Weights of Fluorescent Components in Dissolved Organic Matter Using Asymmetrical Flow Field-Flow Fractionation and Parallel Factor Analysis. *Anal. Chim. Acta* **2012**, *733*, 98−102.
(29) Zhou, Z.; Guo, L. A Critical Evaluation of an Asymmetrical Flow Field-Flow Fractionation System for Colloidal Size Characterization of Natural Organic Matter. *J. Chromatogr. A* **2015**, *1399*, 53−64.
(30) Wünsch, U. J.; Murphy, K. R.; Stedmon, C. A. The One-Sample PARAFAC Approach Reveals Molecular Size Distributions of Fluorescent Components in Dissolved Organic Matter. *Environ. Sci. Technol.* **2017**, *51*, 11900−11908.
(31) Chen, M.; Kim, S.; Park, J.-E.; Jung, H.-J.; Hur, J. Structural and Compositional Changes of Dissolved Organic Matter upon Solid-Phase Extraction Tracked by Multiple Analytical Tools. *Anal. Bioanal. Chem.* **2016**, *408*, 6249−6258.
(32) Guo, L.; Santschi, P. H. Ultrafiltration and Its Applications to Sampling and Characterisation of Aquatic Colloids. In *Environmental Colloids and Particles: Behaviour, Separation and Characterisation*, 2007; pp 159−221.
(33) Lee, M.-H.; Osburn, C. L.; Shin, K.-H.; Hur, J. New Insight into the Applicability of Spectroscopic Indices for Dissolved Organic Matter (DOM) Source Discrimination in Aquatic Systems Affected by Biogeochemical Processes. *Water Res.* **2018**, *147*, 164−176.
(34) Murphy, K. R.; Timko, S. A.; Gonsior, M.; Powers, L. C.; Wünsch, U. J.; Stedmon, C. A. Photochemistry Illuminates Ubiquitous Organic Matter Fluorescence Spectra. *Environ. Sci. Technol.* **2018**, *52*, 11243−11250.
(35) Guo, L.; Santschi, P. H. A Critical Evaluation of the Cross-Flow Ultrafiltration Technique for Sampling Colloidal Organic Carbon in Seawater. *Mar. Chem.* **1996**, *55*, 113−127.
(36) Guo, L.; Santschi, P. H.; Warnken, K. Dynamics of Dissolved Organic Carbon (DOC) in Oceanic Environments. *Limnol. Oceanogr.* **1995**, *40*, 1392−1403.
(37) DeVilbiss, S. E.; Zhou, Z.; Klump, J. V.; Guo, L. Spatiotemporal Variations in the Abundance and Composition of Bulk and Chromophoric Dissolved Organic Matter in Seasonally Hypoxia-Influenced Green Bay, Lake Michigan, USA. *Sci. Total Environ.* **2016**, *565*, 742−757.
(38) Helms, J. R.; Stubbins, A.; Ritchie, J. D.; Minor, E. C.; Kieber, D. J.; Mopper, K. Absorption Spectral Slopes and Slope Ratios as Indicators of Molecular Weight, Source, and Photobleaching of Chromophoric Dissolved Organic Matter. *Limnol. Oceanogr.* **2008**, *53*, 955−969.
(39) Spencer, R. G. M.; Butler, K. D.; Aiken, G. R. Dissolved Organic Carbon and Chromophoric Dissolved Organic Matter Properties of Rivers in the USA. *J. Geophys. Res. Biogeosciences* **2012**, *117*, No. G03001.
(40) Zhou, Z.; Guo, L.; Minor, E. C. Characterization of Bulk and Chromophoric Dissolved Organic Matter in the Laurentian Great Lakes during Summer 2013. *J. Great Lakes Res.* **2016**, *42*, 789−801.
(41) Coble, P. G.; Del Castillo, C. E.; Avril, B. Distribution and Optical Properties of CDOM in the Arabian Sea during the 1995 Southwest Monsoon. *Deep Sea Res., Part II* **1998**, *45*, 2195−2223.
(42) Huguet, A.; Vacher, L.; Relexans, S.; Saubusse, S.; Froidefond, J. M.; Parlanti, E. Properties of Fluorescent Dissolved Organic Matter in the Gironde Estuary. *Org. Geochem.* **2009**, *40*, 706−719.
(43) Zsolnay, A.; Baigar, E.; Jimenez, M.; Steinweg, B.; Saccomandi, F. Differentiating with Fluorescence Spectroscopy the Sources of Dissolved Organic Matter in Soils Subjected to Drying. *Chemosphere* **1999**, *38*, 45−50.
(44) Murphy, K. R.; Stedmon, C. A.; Graeber, D.; Bro, R. Fluorescence Spectroscopy and Multi-Way Techniques. PARAFAC. *Anal. Methods* **2013**, *5*, 6557.
(45) Teber, T. *Seasonal and Spatial Variations in Chemical Composition and Fluxes of Dissolved Organic Matter and Nutrients in the Lower Milwaukee River*; University of Wisconsin: Milwaukee, 2016.
(46) Cai, Y.; Guo, L.; Wang, X.; Aiken, G. Abundance, Stable Isotopic Composition, and Export Fluxes of DOC, POC, and DIC from the Lower Mississippi River during 2006−2008. *J. Geophys. Res.: Biogeosci.* **2015**, *120*, 2273−2288.
(47) Yang, L.; Hong, H.; Guo, W.; Chen, C.-T. A.; Pan, P.-I.; Feng, C.-C. Absorption and Fluorescence of Dissolved Organic Matter in Submarine Hydrothermal Vents off NE Taiwan. *Mar. Chem.* **2012**, *128−129*, 64−71.
(48) von Wandruszka, R. Humic Acids: Their Detergent Qualities and Potential Uses in Pollution Remediation. *Geochem. Trans.* **2000**, *1*, No. 10.
(49) Perminova, I. V.; Frimmel, F. H.; Kudryavtsev, A. V.; Kulikova, N. A.; Abbt-Braun, G.; Hesse, S.; Petrosyan, V. S. Molecular Weight Characteristics of Humic Substances from Different Environments As Determined by Size Exclusion Chromatography and Their Statistical Evaluation. *Environ. Sci. Technol.* **2003**, *37*, 2477−2485.
(50) Guo, W.; Yang, L.; Zhai, W.; Chen, W.; Osburn, C. L.; Huang, X.; Li, Y. Runoff-Mediated Seasonal Oscillation in the Dynamics of Dissolved Organic Matter in Different Branches of a Large Bifurcated Estuary-The Changjiang Estuary. *J. Geophys. Res.: Biogeosci.* **2014**, *119*, 776−793.
(51) Stedmon, C. A.; Markager, S. Resolving the Variability in Dissolved Organic Matter Fluorescence in a Temperate Estuary and Its Catchment Using PARAFAC Analysis. *Limnol. Oceanogr.* **2005**, *50*, 686−697.
(52) Coble, P. G. Characterization of Marine and Terrestrial DOM in Seawater Using Excitation-Emission Matrix Spectroscopy. *Mar. Chem.* **1996**, *51*, 325−346.

https://dx.doi.org/10.1021/acs.est.9b07123
Environ. Sci. Technol. XXXX, XXX, XXX−XXX

(53) Wünsch, U. J.; Stedmon, C. A.; Murphy, K. R.; Bro, R.; Wenig, P. Emerging Patterns in the Global Distribution of Dissolved Organic Matter Fluorescence. *Anal. Methods* **2019**, *11*, 888−893.
(54) Murphy, K. R.; Stedmon, C. A.; Wenig, P.; Bro, R. OpenFluor−an Online Spectral Library of Auto-Fluorescence by Organic Compounds in the Environment. *Anal. Methods* **2014**, *6*, 658−661.

https://dx.doi.org/10.1021/acs.est.9b07123
Environ. Sci. Technol. XXXX, XXX, XXX−XXX